Hydrogen Peroxide Adducts

International Edition: DOI: 10.1002/anie.201606561
German Edition: DOI: 10.1002/ange.201606561

Hydrogen Peroxide Coordination to Cobalt(II) Facilitated by Second-Sphere Hydrogen Bonding

*Christian M. Wallen, Lukáš Palatinus, John Bacsa, and Christopher C. Scarborough**

Abstract: *$M(H_2O_2)$ adducts have been postulated as intermediates in biological and industrial processes; however, only one observable $M(H_2O_2)$ adduct has been reported, where M is redox-inactive zinc. Herein, direct solution-phase detection of an $M(H_2O_2)$ adduct with a redox-active metal, cobalt(II), is described. This $Co^{II}(H_2O_2)$ compound is made observable by incorporating second-sphere hydrogen-bonding interactions between bound H_2O_2 and the supporting ligand, a trianionic trisulfonamido ligand. Thermodynamics of H_2O_2 binding and decay kinetics of the $Co^{II}(H_2O_2)$ species are described, as well as the reaction of this $Co^{II}(H_2O_2)$ species with Group 2 cations.*

Hydrogen peroxide is an attractive and green industrial oxidant that is readily prepared from H_2 and O_2.[1,2] Applications of H_2O_2 include bleaching of cotton and wood pulp[3,4] and oxygenation of propylene to propylene oxide.[5] Oxidations by H_2O_2 often employ metal catalysts, possibly involving $M(H_2O_2)$ intermediates, as such adducts have been computationally[6–9] and kinetically[10–13] implicated. An $Fe^{III}(H_2O_2)$ species has been proposed in cytochromes P450 as or en route to the ill-defined "second oxidant", the key intermediate in a minor oxidation pathway typically overshadowed by the canonical pathway proceeding through Compound I.[14–17] A computational study by Shaik et al.[18] predicted that longevity of $Fe^{III}(H_2O_2)$ adducts in cytochromes P450 is increased when hydrogen-bonding interactions are present between bound H_2O_2 and basic moieties in the active-site pocket (**A**, Figure 1). In 2015, we reported the first $M(H_2O_2)$ adduct, a Zn^{II} species (**B**, Figure 1), made observable by incorporating second-sphere hydrogen-bonding interactions between H_2O_2 and a trianionic trisulfonamido ancillary ligand.[19] Given the presence of a redox-active metal in the putative $Fe^{III}(H_2O_2)$ species in cytochromes P450, we became interested in studying the viability of coordination of H_2O_2 to redox-active metals. Herein, we detail the first observable $M(H_2O_2)$ adduct bearing a redox-active metal.

The disproportionation of H_2O_2 into O_2 and H_2O is accelerated by redox-active metals,[1] so we anticipated that analogues of **B** incorporating redox-active metals would be shorter-lived. We chose to explore a Co^{II} analogue of **B**, as a $Co^{II}(H_2O_2)$ species (**C**, Figure 1) had recently been computationally implicated as reactive for oxidation of hydroquinone to benzoquinone.[9] As described below, our observed $Co^{II}(H_2O_2)$ species is shorter-lived than **B**, but its accessibility corroborates the existence of $M(H_2O_2)$ adducts with redox-active metals and provides a platform for developing catalysts for oxidation reactions with H_2O_2.

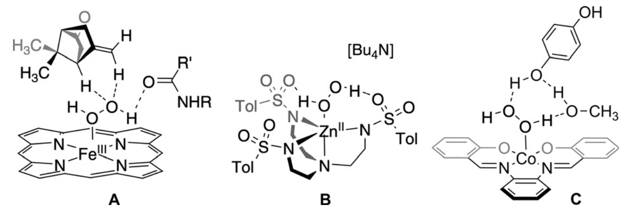

Figure 1. Computed structure[18] demonstrating the importance of hydrogen bonding in an $Fe^{III}(H_2O_2)$ species in cytochromes P450 (**A**); the first H_2O_2 coordination compound (**B**);[19] and a calculated $Co(H_2O_2)$ intermediate in aerobic hydroquinone oxidation (**C**).[9].

We initiated our studies with $[Bu_4N][(Ts_3tren)Co^{II}]$ (**1**) and $[Bu_4N][(Ts_3tren)Co^{II}(OH_2)]$ (**1-OH₂**)[20] (Scheme 1; $(Ts_3tren)^{3-}$ is the ancillary ligand on Zn^{II} in **B**, Figure 1). The H_2O ligand in **1-OH₂** is readily displaced by NH_2OH, N_2H_4, or NH_3 to afford **1-NH₂OH, 1-N₂H₄**, and **1-NH₃**, respectively. X-ray crystallographic characterization of these species[35] revealed the presence of hydrogen-bonding interactions between the sulfonyl oxygen atoms and the axial-ligand protons (Figure 2), including the protons of the distal heteroatom in N_2H_4 and NH_2OH. **1** and **1-OH₂** are differentiated by electronic absorption spectroscopy;[20] however, **1-OH₂** is not distinguishable from its 5-coordinate nitrogenous analogues **1-NH₂OH, 1-N₂H₄**, and **1-NH₃** by this technique

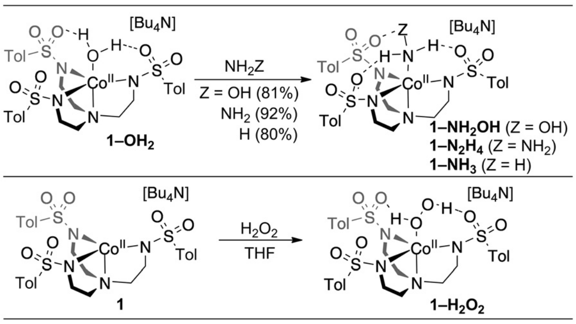

Scheme 1. Synthesis of **1** and **1-L**. Yields are of crystalline product.

---

[*] C. M. Wallen, Dr. J. Bacsa, Prof. Dr. C. C. Scarborough
Department of Chemistry, Emory University
1515 Dickey Dr., Atlanta, GA 30322 (USA)
E-mail: scarborough@emory.edu

Prof. Dr. L. Palatinus
Department of Structure Analysis
Institute of Physics of the AS CR, Prague (Czechia)

Supporting information and the ORCID identification number(s) for the author(s) of this article can be found under http://dx.doi.org/10.1002/anie.201606561.

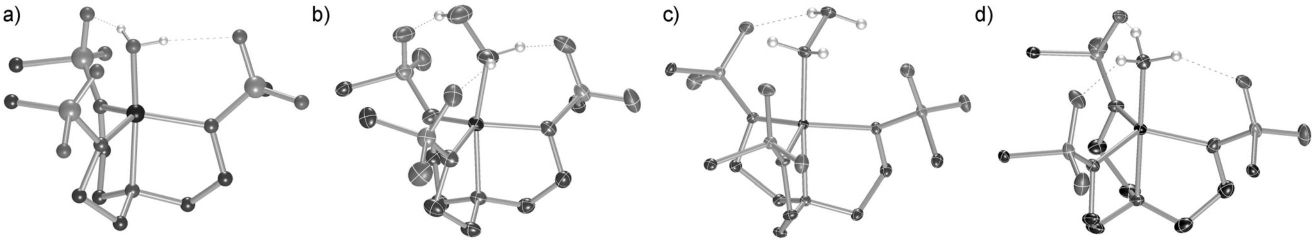

Figure 2. Structures of the anions in **1-OH$_2$** (a), **1-NH$_2$OH** (b), **1-N$_2$H$_4$** (c), and **1-NH$_3$** (d) in the crystalline state, demonstrating intramolecular hydrogen bonding with the axial ligand ($[Bu_4N]^+$ ions omitted).[35] Tolyl groups of the $(Ts_3tren)^{3-}$ ligand are truncated for clarity. Only hydrogen atoms of the axial ligands are shown. **1-OH$_2$**, which is very similar to a complex reported by Borovik et al.,[22] is an incommensurately modulated structure and is therefore represented as a ball-and-stick model.

except by band intensity, where complexes with axial nitrogen ligands show more intense d–d transitions than **1-OH$_2$** (Figure 3).

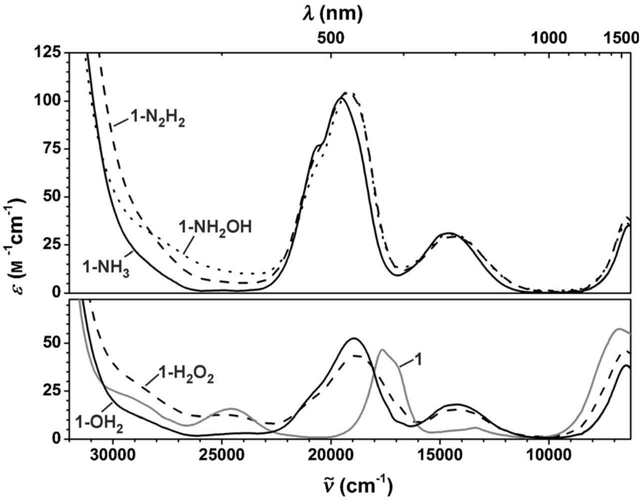

Figure 3. Electronic absorption spectra of **1-NH$_3$**, **1-N$_2$H$_4$**, **1-NH$_2$OH**, **1-OH$_2$**, **1**, and **1-H$_2$O$_2$**.

In 2015, we reported a method for accessing anhydrous H_2O_2 in THF.[19] Although we have not encountered problems with such solutions, they should be handled with care, as formation of radicals and/or organic peroxides is possible, particularly upon heating or irradiation. Addition of anhydrous H_2O_2 in THF to **1-OH$_2$** did not result in any notable changes in the electronic absorption spectrum, and addition of H_2O_2 to **1** provided an absorption spectrum of a five-coordinate Co^{II} species that was indistinguishable from that of **1-OH$_2$** (Figure 3). Despite the redox potential of **1-OH$_2$** (+78 mV vs. Fc/Fc$^+$ in CH_2Cl_2),[20] no cobalt oxidation products were spectroscopically observable on addition of H_2O_2 to **1** or **1-OH$_2$**.[21] Generation of 5-coordinate Co^{II} on addition of H_2O_2 to **1** is consistent with either formation of **1-H$_2$O$_2$** or formation of **1-OH$_2$** as a consequence of immediate H_2O_2 disproportionation by Co^{II}. Distinguishing between these possibilities required a method of directly detecting H_2O_2 in these **1**/H_2O_2 solutions. Despite the paramagnetic nature of the complexes studied, ^{1}H NMR spectroscopy proved a viable technique for studying coordination of H_2O_2 to **1** (Figure 4).

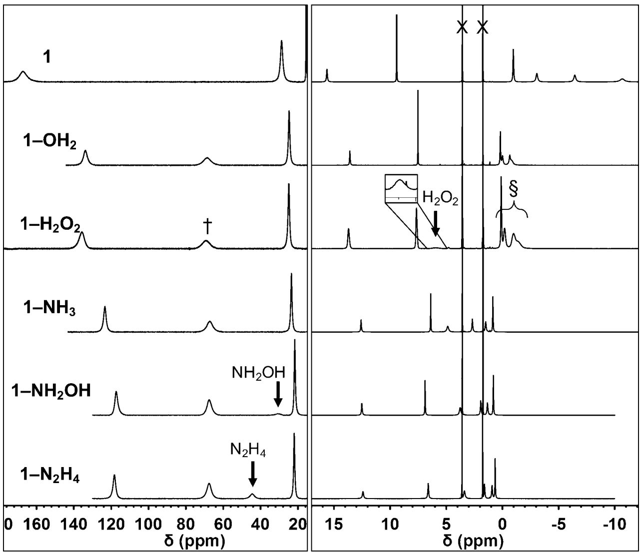

Figure 4. ^{1}H-NMR spectra (in [D$_8$]THF) of cobalt complexes scaled to show resonances for visible axial ligands (N_2H_4, NH_2OH, and H_2O_2), the presence of alkyl-bridge signals in the 5-coordinate complexes (†), and positions of $[Bu_4N]^+$ resonances (§), which are dependent on the number of second-sphere hydrogen bonds (0, 2, or 3). Residual [D$_8$]THF signals are indicated by X.

^{1}H NMR resonances associated with **1-L** were assigned by comparing spectra of related complexes (see the Supporting Information). All 5-coordinate Co^{II} species showed a CH_2 resonance near 65 ppm, and the presence of this signal in a solution containing H_2O_2 and **1** (†, Figure 4) corroborates the electronic absorption data (Figure 3) revealing a 5-coordinate Co^{II} ion. The positions of the Bu proton resonances of the $[Bu_4N]^+$ counterion are affected by the presence of axial ligands on cobalt. In the ^{1}H NMR spectrum of **1**, the Bu signals are spaced between 1 and −11 ppm, where the large paramagnetic shifting is consistent with interaction between the $[Bu_4N]^+$ cation and the cobalt complex in solution, likely through hydrogen bonding between the α-hydrogen atoms on Bu and the sulfonyl oxygen atoms as seen in the solid state. For derivatives **1-L** with three second-sphere hydrogen bonds (**1-NH$_2$OH**, **1-NH$_3$**, and **1-N$_2$H$_4$**) the Bu signals are less paramagnetically shifted (0 to 5 ppm), consistent with axial coordination disrupting hydrogen bonding between the ions in solution. For **1-OH$_2$**, which only contains two second-sphere hydrogen bonds, the Bu proton resonances overlap between 1 and −1 ppm. When anhydrous H_2O_2 is combined with **1**, the Bu proton resonances appear between 1 and −2 ppm, similar to **1-OH$_2$** (§, Figure 4). These data suggest that the axial ligand in a solution of **1** and anhydrous H_2O_2 is diprotic, which could be explained by binding of H_2O or H_2O_2. For complexes **1-OH$_2$** and **1-NH$_3$**, the proton resonances corresponding to the axial ligand are not observable by ^{1}H NMR spectroscopy, even upon addition of excess ligand (see the Supporting Information). However, ^{1}H NMR spectra of **1-N$_2$H$_4$** and **1-NH$_2$OH** show signals at 44 ppm and 30 ppm, respectively, corresponding to the axial-ligand protons (Figure 4). The spectrum of a solution of **1** and anhydrous H_2O_2 contains a broad signal at 5.9 ppm (Figure 4). Over time, this signal shifts to 8.8 ppm (closer to that of free H_2O_2 at 9.4 ppm) and decreases in intensity following a first-order pathway with a half-life of (353 ± 33) s (Figure 5). This shifted H_2O_2 resonance is the first direct evidence that H_2O_2 is binding to Co^{II} in **1**, as the ^{1}H NMR and electronic spectra demonstrate that Co^{II} is five-coordinate under these conditions. The decay product of **1-H$_2$O$_2$** was identified as **1-OH$_2$** by crystallization of the bulk material. The shifting H_2O_2 resonance throughout decay of **1-H$_2$O$_2$** points to an equilibrium between free and bound H_2O_2 that is perturbed by H_2O formed upon H_2O_2 disproportionation, leading us to examine the equilibrium constants of binding H_2O_2 and H_2O to **1**.

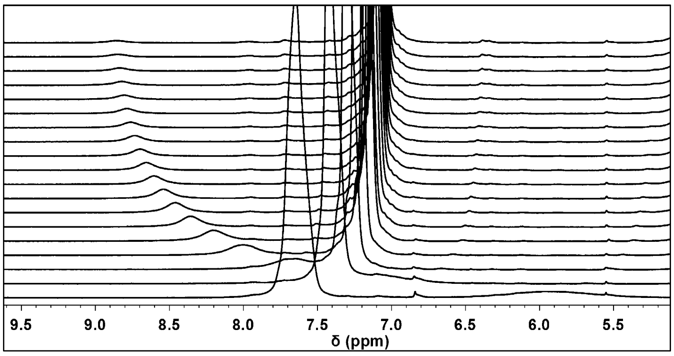

Figure 5. Room-temperature decay of **1-H$_2$O$_2$** measured by ^{1}H NMR spectroscopy (in [D$_8$]THF). The H_2O_2 resonance shifts from 5.9 ppm to 8.8 ppm. The decay product was confirmed by X-ray crystallography to be **1-OH$_2$**.[35] The tall signal at 7.7 ppm shifting to 7.1 ppm is a methyl group on the sulfonamidate ligand.

To probe whether H_2O_2 binding is perturbed by the presence of H_2O, H_2O_2 was added to **1-OH$_2$** and its decay monitored by ^{1}H NMR spectroscopy. Initially, the H_2O_2 resonance appeared at 8.8 ppm (c.f. 5.9 ppm in the absence of H_2O) and then shifted toward 9.1 ppm [$t_{1/2}$ = (1190 ± 10) s]. When H_2O_2 was added to **1-NH$_3$**, the H_2O_2 resonance remained at 9.5 ppm and decayed with a half-life of (13700 ± 200) s. These data are consistent with H_2O_2 disproportionation occurring upon coordination to **1**, and with H_2O_2 being a weaker ligand for **1** than H_2O or NH_3, consistent with descriptions of H_2O_2 as a very poor ligand.[23–27] The first-order decay of **1-H$_2$O$_2$** contrasts the second-order decay mechanism of **B**, which bears the same ligand and counterion, and at the same starting concentration has a half-life of 10^4 s.[19] This comparison suggests that the redox-active nature of M has a dramatic effect on the stability of M(H_2O_2) species.

We sought to quantify binding affinities of **1** for H_2O and H_2O_2. H_2O_2 has been described as a poor ligand[23–27] such that its coordination to metals was not unambiguously detected until 2015.[19] Prikhodchenko et al. demonstrated that H_2O_2 is a more effective hydrogen-bond donor than H_2O, clarifying the importance of second-sphere hydrogen bonding in H_2O_2 coordination.[27–30] Because of the short lifetime of **1-H$_2$O$_2$**, we turned to photometric titrations using electronic absorption spectroscopy to determine the binding constants for H_2O and H_2O_2 to **1** at −70 °C, as decay of **1-H$_2$O$_2$** cannot be detected within one hour at temperatures below −40 °C by NMR spectroscopy. Titration of **1** with H_2O or anhydrous H_2O_2 in THF at −70 °C afforded the curves shown in Figure 6, from which K_{eq} values for the coordination of H_2O_2 and H_2O to **1** are derived: (31.3 ± 0.2) M^{-1} and (31600 ± 12600) M^{-1} at −70 °C, respectively. These data establish a preference for binding of **1** to H_2O over H_2O_2, where K_{eq} for displacing H_2O_2 in **1-H$_2$O$_2$** by H_2O at −70 °C is (1010 ± 400) ($\Delta G = -2.8$ kcal mol^{-1}). To our knowledge, this is the first H_2O_2/metal binding constant measured.

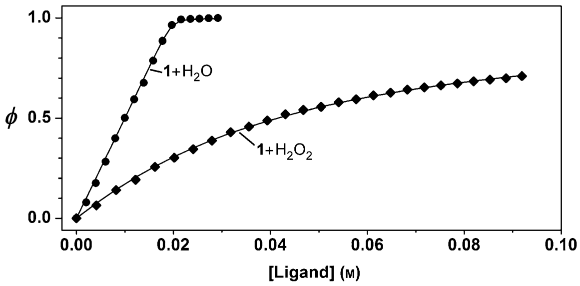

Figure 6. Photometric titrations of **1** with H_2O and H_2O_2 in THF at −70 °C. Data are plotted as fractional saturation vs. concentration of the ligand (H_2O or H_2O_2). The curves, which are nonlinear fits to the data, enable calculation of K_{eq} [(3.16 ± 1.26) × 10^4 M^{-1} for H_2O and (31.3 ± 0.2) M^{-1} for H_2O_2).

Finally, we probed the reactivity of **1-H$_2$O$_2$**. Borovik et al. reported that a species closely related to **1** is inert to PhIO, but upon addition of Group 2 ions, oxidation of the Co^{II} center by PhIO afforded an isolable Co^{III}(μ-OH)Ca^{2+} species.[22] This transformation may involve a transient Co^{IV} intermediate, as redox-inert cations are known to facilitate two-electron oxidation of Co^{II} to Co^{IV}.[31,32] We probed whether Group 2 ions could similarly promote cobalt oxidation and cleavage of the O–O bond of H_2O_2 in **1-H$_2$O$_2$**. We have shown that **1** and related species react readily with Group 2 ions to afford heterotrimetallic sandwich compounds.[20] Addition of M(OTf)$_2$ (M = Ca^{2+}, Sr^{2+}, or Ba^{2+}) to **1-H$_2$O$_2$** resulted in rapid conversion into intensely green products, each with nearly identical electronic absorption spectra. The spectroscopic properties of these green species did not satisfactorily agree with Borovik's report of a red-brown Co^{III}(μ-OH)Ca^{2+} species;[22] however, combination of [(15-crown-5)Ca](OTf)$_2$

and **1-H_2O_2** afforded X-ray-quality crystals of a Co^{III}(μ-OH)Ca^{2+} complex (**2**, Scheme 2),[35] demonstrating Group 2 ion induced oxidation of Co^{II} to Co^{III} by H_2O_2. The oxidation potential of **1-OH_2** is +78 mV vs. Fc/Fc^+ in CH_2Cl_2,[20] so the oxidative stability of the Co^{II} ion in **1-H_2O_2** suggests that one-electron redox processes involving **1-H_2O_2** are not preferred.

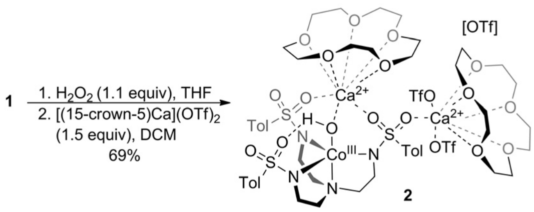

Scheme 2. Reaction of **1-H_2O_2** with Ca^{2+} to form **2**. The crystal structure analysis of **2** is included in the Supporting Information. DCM: dichloromethane.

We expect that the Group 2 ions are brought into close proximity with coordinated H_2O_2 in **1-H_2O_2**, as we[20] and Borovik et al.[22,33] have shown that such sulfonyl oxygen atoms bind Group 2 metal ions without significantly impacting the electronic properties of Co^{II}. We hypothesize that the Group 2 ion induced oxidative conversion of **1-H_2O_2** into **2** may involve a transient Co^{IV}(oxo)/Ca^{2+}(OH_2) or Co^{IV}(OH)/Ca^{2+}(OH) species that rapidly reacts with a hydrogen-atom donor, likely THF, to afford the observed Co^{III} species **2**. Rapid decomposition of Co^{IV} has been demonstrated in the instability of related Co^{IV}(oxo)[22,31,32] and Co^{IV}(nitrido)[34] species. Regardless of mechanism, the Group 2 ion induced conversion of **1-H_2O_2** into **2** provides a new approach to H_2O_2 activation involving coordination to one metal center and activation by a second metal center. We are currently exploring this dual activation of H_2O_2 for use in oxidation catalysis.

In summary, we have obtained the first direct evidence for formation of an M(H_2O_2) complex with a redox-active metal. Mixing **1** and anhydrous H_2O_2 resulted in coordination of an axial ligand to cobalt(II) at temperatures where H_2O_2 is not disproportionated by **1**, and low-temperature photometric titration of **1** with H_2O_2 or H_2O, as well as decay kinetics of **1-H_2O_2** in the presence of H_2O, revealed that H_2O_2 is a weaker ligand for the Co^{II} center in **1** than H_2O. **1-H_2O_2** is stable to oxidation of the Co^{II} center, but addition of [(15-crown-5)Ca]$(OTf)_2$ induced oxidation to afford the Co^{III}(μ-OH)Ca^{2+} complex **2**. Activation of coordinated H_2O_2 by a secondary metal is a novel approach to developing oxidation reactions with H_2O_2, and our efforts on expanding the coordination chemistry of H_2O_2 and exploiting the reactivity of M(H_2O_2) adducts are on-going.

Acknowledgements

This work was enabled by funds from a National Science Foundation CAREER award (CHE-1455211).

Keywords: cobalt · hydrogen bonds · peroxides · peroxido ligands · second-sphere interactions

How to cite: *Angew. Chem. Int. Ed.* **2016**, *55*, 11902–11906
Angew. Chem. **2016**, *128*, 12081–12085

---

[1] C. W. Jones, *Applications of Hydrogen Peroxide and Derivatives*, Royal Society, Cambridge, UK, **1999**.
[2] M. Lancaster, *Green Chemistry*, Royal Society, Cambridge, UK, **2002**.
[3] R. Hage, J. W. de Boer, F. Gaulard, K. Maaijen, *Adv. Inorg. Chem.* **2013**, *65*, 85–116.
[4] R. Hage, A. Lienke, *Angew. Chem. Int. Ed.* **2006**, *45*, 206–222; *Angew. Chem.* **2006**, *118*, 212–229.
[5] V. Russo, R. Tesser, E. Santacesaria, M. Di Serio, *Ind. Eng. Chem. Res.* **2013**, *52*, 1168–1178.
[6] M. Chen, Y. Pan, H.-K. Kwong, R. J. Zeng, K.-C. Lau, T.-C. Lau, *Chem. Commun.* **2015**, *51*, 13686–13689.
[7] H.-K. Kwong, P.-K. Lo, K.-C. Lau, T.-C. Lau, *Chem. Commun.* **2011**, *47*, 4273–4275.
[8] L. Ma, Y. Pan, W.-L. Man, H.-K. Kwong, W. W. Y. Lam, G. Chen, K.-C. Lau, T.-C. Lau, *J. Am. Chem. Soc.* **2014**, *136*, 7680–7687.
[9] C. W. Anson, S. Ghosh, S. Hammes-Schiffer, S. S. Stahl, *J. Am. Chem. Soc.* **2016**, *138*, 4186–4193.
[10] P. Afanasiev, E. V. Kudrik, J.-M. M. Millet, D. Bouchu, A. B. Sorokin, *Dalton Trans.* **2011**, *40*, 701–710.
[11] S. A. Mirza, B. Bocquet, C. Robyr, S. Thomi, A. F. Williams, *Inorg. Chem.* **1996**, *35*, 1332–1337.
[12] A. Theodoridis, J. Maigut, R. Puchta, E. V. Kudrik, R. van Eldik, *Inorg. Chem.* **2008**, *47*, 2994–3013.
[13] M. Wolak, R. van Eldik, *Chem. Eur. J.* **2007**, *13*, 4873–4883.
[14] M. J. Coon, *Annu. Rev. Pharmacol. Toxicol.* **2005**, *45*, 1–25.
[15] I. G. Denisov, T. M. Makris, S. G. Sligar, I. Schlichting, *Chem. Rev.* **2005**, *105*, 2253–2278.
[16] *Cytochrome P450: Structure, Mechanism, and Biochemistry* (Ed.: P. R. Ortiz de Montellano), Kluwer Academic/Plenum Publishers, New York, **2005**.
[17] S. Shaik, D. Kumar, S. P. de Visser, A. Altun, W. Thiel, *Chem. Rev.* **2005**, *105*, 2279–2328.
[18] B. Wang, C. Li, K. D. Dubey, S. Shaik, *J. Am. Chem. Soc.* **2015**, *137*, 7379–7390.
[19] C. M. Wallen, J. Bacsa, C. C. Scarborough, *J. Am. Chem. Soc.* **2015**, *137*, 14606–14609.
[20] C. M. Wallen, M. Wielizcko, J. Bacsa, C. C. Scarborough, *Inorg. Chem. Front.* **2016**, *3*, 142–149.
[21] Since related Co^{III} species display intense electronic transitions in the visible region,[31] the presence of >0.1% Co^{III} would be visible by electronic absorption spectroscopy in solutions of **1** and H_2O_2.
[22] D. C. Lacy, Y. J. Park, J. W. Ziller, J. Yano, A. S. Borovik, *J. Am. Chem. Soc.* **2012**, *134*, 17526–17535.
[23] A. G. DiPasquale, J. M. Mayer, *J. Am. Chem. Soc.* **2008**, *130*, 1812–1813.
[24] A. G. Medvedev, A. A. Mikhaylov, A. V. Churakov, M. V. Vener, T. A. Tripol'skaya, S. Cohen, O. Lev, P. V. Prikhodchenko, *Inorg. Chem.* **2015**, *54*, 8058–8065.
[25] A. A. Mikhaylov, A. G. Medvedev, A. V. Churakov, D. A. Grishanov, P. V. Prikhodchenko, O. Lev, *Chem. Eur. J.* **2016**, *22*, 2980–2986.
[26] A. V. Churakov, S. Sladkevich, O. Lev, T. A. Tripol'skaya, P. V. Prikhodchenko, *Inorg. Chem.* **2010**, *49*, 4762–4764.
[27] Y. Wolanov, A. Shurki, P. V. Prikhodchenko, T. A. Tripol'skaya, V. M. Novotortsev, R. Pedahzur, O. Lev, *Dalton Trans.* **2014**, *43*, 16614–16625.
[28] A. V. Churakov, P. V. Prikhodchenko, J. A. K. Howard, O. Lev, *Chem. Commun.* **2009**, 4224–4226.

[29] P. V. Prikhodchenko, A. G. Medvedev, T. A. Tripol'skaya, A. V. Churakov, Y. Wolanov, J. A. K. Howard, O. Lev, *CrystEngComm* **2011**, *13*, 2399 – 2407.

[30] M. V. Vener, A. G. Medvedev, A. V. Churakov, P. V. Prikhodchenko, T. A. Tripol'skaya, O. Lev, *J. Phys. Chem. A* **2011**, *115*, 13657 – 13663.

[31] S. Hong, F. F. Pfaff, E. Kwon, Y. Wang, M.-S. Seo, E. Bill, K. Ray, W. Nam, *Angew. Chem. Int. Ed.* **2014**, *53*, 10403 – 10407; *Angew. Chem.* **2014**, *126*, 10571 – 10575.

[32] F. F. Pfaff, S. Kundu, M. Risch, S. Pandian, F. Heims, I. Pryjomska-Ray, P. Haack, R. Metzinger, E. Bill, H. Dau, P. Comba, K. Ray, *Angew. Chem. Int. Ed.* **2011**, *50*, 1711 – 1715; *Angew. Chem.* **2011**, *123*, 1749 – 1753.

[33] S. A. Cook, A. S. Borovik, *Acc. Chem. Res.* **2015**, *48*, 2407 – 2414.

[34] E. M. Zolnhofer, M. Käß, M. M. Khusniyarov, F. W. Heinemann, L. Maron, M. van Gastel, E. Bill, K. Meyer, *J. Am. Chem. Soc.* **2014**, *136*, 15072 – 15078.

[35] CCDC 144760 (**1-OH$_2$**), 144761 (**1-N$_2$H$_4$**), 144762 (**1-NH$_2$OH**), 144763 (**2**), and 1489712 (**1-NH$_3$**) contain the supplementary crystallographic data for this paper. These data can be obtained free of charge from The Cambridge Crystallographic Data Centre.

Received: July 6, 2016